Comparison of Constant and Temperature Dependent Blood Perfusion in Temperature Prediction for Superficial Hyperthermia

Tomáš DŘÍŽĎAL[1,2], Paolo TOGNI[1,2], Lukáš VÍŠEK[1], Jan VRBA[1]

[1]Dept. of Electromagnetic Field, Czech Technical Univ in Prague, Technicka 2, 166 27 Prague, Czech Republic
[2]Dept. of Radiotherapy, ErasmusMC - Daniel den Hoed, Groenehilledijk 301, 3075 EA Rotterdam, The Netherlands

t.drizdal@erasmusmc.nl, p.togni@erasmusmc.nl, visekluk@fel.cvut.cz, vrba@fel.cvut.cz

Abstract. *The purpose of this study was to determine whether prediction of the 3D temperature profile for superficial hyperthermia using constant blood perfusion model could be matched to one with a temperature dependent blood perfusion. We compared three different constant blood perfusion scenarios with one temperature dependent blood perfusion using a layered model of biological tissue consisting of skin (2 mm), fat (10 mm) and muscle (108 mm). For all four scenarios the maximum temperature of 43 °C was found in the muscle tissue in the close proximity (1 – 3 mm) of fat layer. Cumulative histograms of temperature versus volume were identical for the region of 100x100x40* mm^3 *under the applicator aperture for the three constant blood perfusion models. For temperature dependent blood perfusion model, 85 % of the studied region was covered with the temperature equal or higher than 40 °C in comparison with 43 % for the constant blood perfusion models. Hence this study demonstrates that constant blood perfusion scenarios cannot be matched to one with a temperature dependent blood perfusion.*

Keywords

Superficial hyperthermia, bioheat equation, blood perfusion, SAR, temperature prediction.

1. Introduction

Superficial hyperthermia is a therapeutic application of heat to treat cancer diseases at the surface of human body. Several clinical trials have shown the benefit of adding hyperthermia to the radiotherapy treatment, especially for the recurrent diseases where proper radiotherapy dose could not be reached due to the previous radiation [1] - [5]. The temperatures during the hyperthermia treatment are measured inside interstitial catheters (if possible) and at the body surface. Conformal thermal monitoring sensor array sheet can be used for the accurate surface temperature monitoring during the entire treatment [6]. Power generators controlled with respect to actual temperature in treated region are turned off in case the maximal temperature in healthy tissue exceeds 43 – 44 °C or patient complaints. Since the invasive number of thermometry sites is in general very limited (1 – 4 probes with several measurements points) and the surface measurements are influenced by the water bolus temperature, patient specific 3D SAR (specific absorption rate) and temperature prediction become of great importance. Such models provide us with detailed information about the 3D SAR and temperature distribution in the treated area and might help to minimize the presence of hot-spots (area with high local temperature) in regions that are not monitored by interstitial thermometry [7], [8].

Electromagnetic energy radiated from external antennas (applicators) increases temperature in the treated area to the therapeutic level of 40 – 43 °C. The applicators usually work at frequencies of 434 MHz or 915 MHz [9]. Lucite cone applicator (LCA) and contact flexible microstrip applicator (CFMA) are examples of 434 MHz applicators currently used in clinical practice [10]-[13]. Dual-arm archimedean spiral array and dual concentric conductor microstrip antenna represent planar applicators working at 915 MHz [14], [15]. Wieringen et al. developed also CFMA operating at 70 MHz for the treatment of deeper situated tumors [16].

To develop a process for hyperthermia treatment modeling based on thermal dose, it is required to correctly transform the 3D SAR distribution into 3D temperature distribution. A proper implementation of energy transport caused by blood perfusion is essential to estimate the temperature distribution. Therefore in this study we focused our attention especially on the necessity to consider blood perfusion as a temperature dependent quantity. The heat transfer problem inside a biological tissue can be described using bioheat equation (BHTE) which was first introduced by Pennes [17]:

$$c\,\rho\,\frac{\partial T}{\partial t} = k\,\nabla^2\,T - c_b\,W\,(T - T_b) + \rho\,\mathrm{SAR} \qquad (1)$$

where c (J kg^{-1}K^{-1}) represents specific heat capacity, ρ (kg m^{-3}) density, k (W m^{-1}K^{-1}) represents thermal con-

ductivity, c_b (J kg^{-1}K^{-1}) represents specific heat capacity of blood, W (kg m^{-3}s^{-1}) blood perfusion rate and T_b (K) temperature of the circulated blood. The absorbed energy from the electromagnetic field simulation represented by SAR (W kg^{-1}) was used as a source for thermal calculations. Crezee et al. [18] showed the limitations of BHTE predicting temperature profile in presence of large artificial vessels.

Lang et al. [19] compared temperature dependent and constant blood perfusion for regional hyperthermia. To model temperature dependent blood perfusion, they used special functions for fat, muscle and tumour which follow in temperature range of 37 °C - 44 °C behaviors introduced by Song et. al [20]. They found that temperature dependent blood perfusion model predicts much larger amount of muscle tissue heated above 40 °C. It was also shown that significantly lower amount of power (340 W versus 430 W) was needed for temperature dependent blood perfusion model to achieve 3D temperature distribution limited by the maximum of 44 °C in healthy tissue.

Prediction of 3D temperature profile using temperature dependent blood perfusion is a highly nonlinear problem resulting in higher computation requirements than usage of constant blood perfusion. If constant blood perfusion could be used for temperature prediction it may save computation time. Since the implementation of thermal dependent blood perfusion models is not common among hyperthermia treatment planning packages, this study provides information about the necessity to implement such features. The purpose of this study was to address following question: Can we match prediction of 3D temperature profile for superficial hyperthermia using constant and temperature dependent blood perfusion?

For the temperature dependent blood perfusion model we tuned the applicator input power to reach a maximum temperature of 43 °C inside the layered model of biological tissue. Subsequently we recalculated the identical model differing in constant blood perfusion and compared maximal temperatures with first scenario. As constant values for blood perfusion we used tabled literature values (Tab. 1). In the second step we tuned also input powers for constant blood perfusion models to reach 43 °C and compared their temperature distributions.

2. Materials and Methods

For this study we chose COMSOL Multiphysics [21] as a simulation package considering coupling of electromagnetic field and thermal problems together with nonlinear behavior for blood perfusion. To decrease computation requirements we calculated the electromagnetic field and the thermal simulations independently. A common electromagnetic field simulation stored in memory was used for all thermal calculations. Variation of the input power to reach the required values was done by scaling the SAR term within BHTE. All thermal calculations were done for the steady state situation where the whole process was in thermal equilibrium.

2.1 3D Model

The applicator selected for this study was designed to operate at 434 MHz and it was similar to that introduced by Rhoon et al. [10]. The waveguide geometrical dimensions (width 60 mm, height 30 mm, length 72 mm) were calculated in order to excite single TE_{10} mode. To decrease the cut off frequency and to reduce the geometrical dimensions the applicator was filled with deionized water. The feeding of the applicator was provided by a $\frac{\lambda}{4}$ (25 mm) monopole antenna placed 15 mm from the back (short) side of the waveguide. To achieve a more uniform distribution of the electromagnetic field inside the horn aperture, the two brass walls parallel to the direction of the E-field were replaced by Lucite (thickness 2 mm). The Lucite horn was chosen 75 mm long with a final aperture of 100x100 mm^2 (inner dimensions) see Fig. 1.

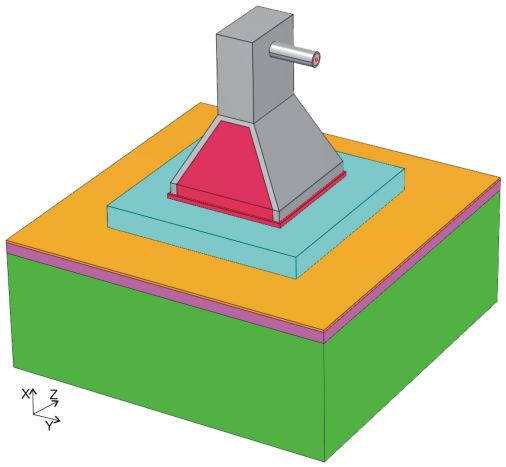

Fig. 1. Model of Lucite applicator in COMSOL Multiphysics.

We used biological tissue model with similar geometrical dimensions as considered the water bolus temperature guideline by Gaag et al. [22]. The model consisted of skin (2 mm), fat (10 mm) and muscle (108 mm) where the area under the aperture was squared (300x300 mm^2). We extended the thickness of skin layer over 1 mm to avoid presence of small grid elements necessary to describe thin layers in the finite element method (FEM) mesh. Between the horn aperture and the surface of the layered tissue model we placed a 180x180x20 mm^3 water bolus with circulated deionized water set to specified temperature (precise value depends on the treatment target depths) [22], [23]. Dielectric and thermal properties of biological tissues at frequency of 434 MHz, for temperature of 37 °C respectively, are listed in Tab. 1.

Material	ε_r $(-)$	σ $(\frac{S}{m})$	ρ $(\frac{kg}{m^3})$	c $(\frac{J}{kg\,K})$	k $(\frac{W}{m\,K})$	W $(\frac{kg}{m^3\,s})$
Deionized water	78	0.046	-	-	-	-
Lucite	2.6	0.003	-	-	-	-
Skin(wet)	49	0.68	1040	3662	0.34	0.45
Fat	5.6	0.042	888	2387	0.22	0.36
Muscle	57	0.8	1050	3639	0.56	0.45
Blood	-	-	1043	3825	-	-

Tab. 1. Dielectric properties at 434 MHz [24], thermal properties for 37 °C [25], [22].

2.2 Simulation Setup

For the electromagnetic field simulation we placed extra air around the antenna and assigned all borders of the entire model as scattering boundary conditions. To decrease the amount of tetrahedral elements describing the applicator geometry we modeled all metal parts as perfect electric conductor (PEC) boundary conditions. The detailed information about the grid settings for all objects are summarized in Tab. 2. Inside the muscle layer we refined a region of 100x100x28 mm^3 with finer grid step (second values in Tab. 2).

Model name	Tetrahedral elements	Maximum size (mm)	Maximal growth rate (-)
Air	93 006	50	1.3
Teflon	5 652	5	1.3
Coaxial inner	1 550	1.5	-
Water applicator	34 586	10	1.2
Lucite	4 746	-	-
Water bolus	20 097	10	1.2
Skin	19 844	-	-
Fat	32 803	8	1.3
Muscle	60 467	25/8	1.3/1.2

Tab. 2. Grid settings for all objects present in model.

For all our analyzes in this study we normalized the incident power P_{inc} (W) (power entering into the calculating domain) to 1 W. That means we neglected the reflections caused by non-perfect impedance matching. This normalization could be useful for some sensitivity analyses where the applicator impedance matching is changing - e.g. influence of fat layer thickness on 3D SAR distribution. P_{inc} can be expressed as follows

$$P_{inc} = P - P_{ref} = P\left(1 - {S_{11}}^2\right) \tag{2}$$

where P (W) is input power, P_{ref} (W) is the reflected power and S_{11} $(-)$ is input voltage reflection coefficient. We calculated power losses individually for all objects (including absorption inside boundaries). The sum of all power losses should be equal to P_{inc} (1 W for our case).

The computational domain of the thermal distribution simulations was reduced including the layered model of biological tissue. Gaag et al. [22] found that the influence of the water bolus with dimensions of 180x180x10 mm^3 can be described with a heat transfer coefficient h = 152 W m^{-2}K^{-1}. Because of this we used a similar water bolus but with 20 mm thickness. We modeled the presence of the water bolus as a boundary condition with identical heat transfer coefficient and $T_{external} = 37$ °C. All other boundaries at the border of model and initial temperatures of all objects at the beginning of the simulations were set to 37 °C. Influence of the water bolus temperature $(T_{external})$ was not an objective of this study.

2.3 Temperature Dependent Blood Perfusion

Several experiments have shown that the response of vasculature system to heat stress is strongly temperature dependent [20]. To describe the temperature dependence of blood perfusion for fat and muscle tissue we followed expressions introduced by Lang et al. [19]. For the blood perfusion of skin we overlapped the curve from [20] by the similar analytical expression as used for fat and muscle. To clearly describe the differences among the tissues and to separate the constant and temperature dependent part of blood perfusion we created a Scaling Function (SF). The value of SF for every tissue in the model was normalized to the temperature of 37 °C. Using this technique the blood perfusion term in BHTE became $SF\,c_b W\,(T - T_b)$. SF for skin, fat and muscle tissue can be expressed as follows

$$SF_{s(T)} = \begin{cases} 1 + 9.2\,exp\left(-\frac{(T-44)^2}{10}\right) & \mathrm{T} \le 44\,^{\circ}\mathrm{C}, \\ 10.2 & \mathrm{T} > 44\,^{\circ}\mathrm{C}, \end{cases} \tag{3}$$

$$SF_{f(T)} = \begin{cases} 1 + exp\left(-\frac{(T-45)^2}{12}\right) & \mathrm{T} \le 45\,^{\circ}\mathrm{C}, \\ 2 & \mathrm{T} > 45\,^{\circ}\mathrm{C}, \end{cases} \tag{4}$$

$$SF_{m(T)} = \begin{cases} 1 + 7.9\,exp\left(-\frac{(T-45)^2}{12}\right) & \mathrm{T} \le 45\,^{\circ}\mathrm{C}, \\ 8.9 & \mathrm{T} > 45\,^{\circ}\mathrm{C}. \end{cases} \tag{5}$$

A graphical representation of (3) – (5) is shown in Fig. 2.

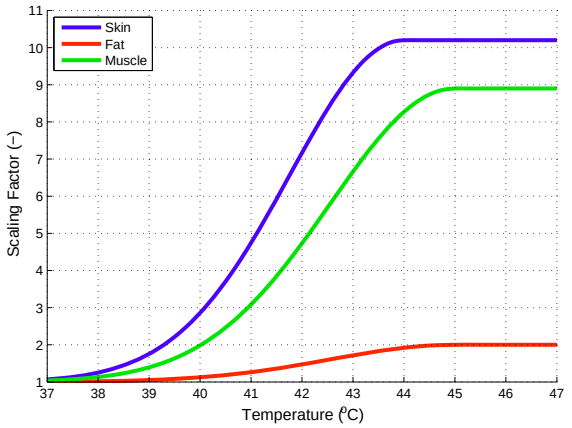

Fig. 2. Perfusion scaling factors for the layered model of biological tissue.

2.4 Studied Scenarios for Blood Perfusion

We studied one temperature dependent scenario and three scenarios with constant blood perfusion scaled to appropriate temperatures.

- **scenario 1** - blood perfusion of skin, fat and muscle were temperature dependent (the blood perfusion values were changed locally with respect to the actual temperature),
- **scenario 2** - all blood perfusion was treated as constants and values were scaled to 43 °C of temperature dependent behaviors,
- **scenario 3** - this scenario was proposed by Kumaradas et al. [26]. Because the skin layer was cooled by water bolus, it was estimated to remain at a body temperature of 37 °C. Fat layer was assumed to reach the temperature of 41 °C and the muscle was estimated to be heated to target temperature of 43 °C. Constant blood perfusion of the respective tissues was scaled to these temperatures,
- **scenario 4** - Lang et al. [19] used for calculation of constant blood perfusion average values of all tissues in the temperature interval of 37 – 43 °C. With respect to (3) – (5) we calculated mean values for all SF (scaling functions) and afterwards found corresponding temperatures used for scaling (skin – 41.18 °C, fat – 41.49 °C, muscle – 41.49 °C).

All the studied scenarios are summarized in Tab. 3. Blood perfusion for the first scenario is equal to the value for 37 °C (e.g. $W_{skin} = 0.45$ kg m^{-3}s^{-1}, see Tab. 1) scaled with temperature dependent $SF_{S(T)}$. For the scenarios 2 – 4 we calculated blood perfusion as e.g. for scenario no. 4

$$W_{skin} = W_{skin(37^oC)}\ SF_{s(41.18)} = 0.45\ 5.16 = 2.32\ \frac{\text{kg}}{\text{m}^3\ \text{s}} \quad (6)$$

Scenario	W_{skin} $(\frac{\text{kg}}{\text{m}^3\ \text{s}})$	W_{fat} $(\frac{\text{kg}}{\text{m}^3\ \text{s}})$	W_{muscle} $(\frac{\text{kg}}{\text{m}^3\ \text{s}})$
1	$0.45\ SF_{s(T)}$	$0.36\ SF_{f(T)}$	$0.45\ SF_{m(T)}$
2	4.19	0.62	3
3	0.45	0.46	3
4	2.32	0.49	1.72

Tab. 3. Studied scenarios for blood perfusion.

As a reference for the evaluation, we used the model with temperature dependent blood perfusion (scenario 1). For this model we tuned input power to reach maximum of 43 °C. Afterwards we applied identical power settings for other 3 scenarios and compared their cumulative temperature-volume histograms (similar to those used by Gaag et al. [22]) in the region of interest (100x100x40 mm^3). Cumulative temperature-volume histograms clearly describe the coverage of selected region (volume) with certain temperature iso-surface. The region was defined by inner dimensions of the applicator aperture and depth of 4 cm from the surface, which represents the maximal depth of the superficial hyperthermia treatment at 434 MHz.

In the second step we tuned the input power for the models with constant blood perfusion in order to reach the maximum temperature of 43 °C and again for the mentioned region comparing cumulative temperature-volume histograms. We also compared cross-sections for the X direction and Y, Z directions (parallel to the applicator aperture) in the depth, where the maximum temperature of 43 °C was reached.

3. Results

3.1 Power Loses in Calculation Domain

From the 3D electromagnetic field distribution we calculated power losses for every part of the model (P_{inc} was normalized to 1 W using equation 2), see Tab. 4. 513 mW (51.3 %) of the power entering the calculation domain was absorbed inside the deionized water filling of the applicator. The sum of the power losses inside the biological tissue equivalent phantom was 0.370 W, representing the amount of power used for thermal calculations. We considered the difference between the total losses in entire calculation domain (0.985 W) and P_{inc} (1W) as the error of the electromagnetic field calculation (0.015 W = 1.5 %).

Object	Power loss (mW)	Object	Power loss (mW)
Water applicator	513	Teflon	3.3
Lucite	45.6	Water bolus	21
Skin	49.6	Fat	29.9
Muscle	290.2	Boundary	32.5

Tab. 4. Power losses (mW) for normalization to 1 W of incident power P_{inc}.

3.2 SAR Distribution

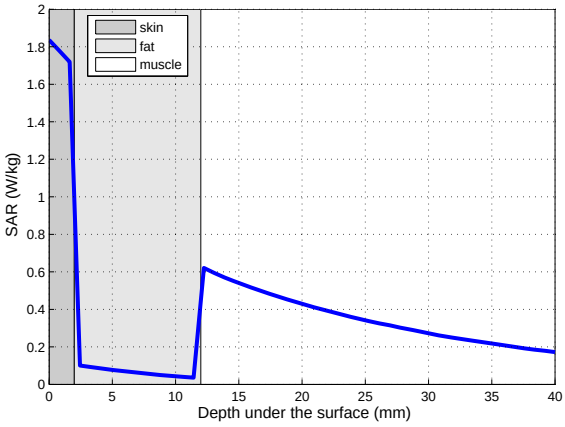

Fig. 3. SAR distribution along central X axis of the applicator, normalized to $P_{inc} = 1$ W.

The SAR distribution along the X axis normalized to P_{inc} = 1 W is shown in Fig. 3. Maximum SAR = 1.83 W/kg

was found at the surface of the skin layer. Absorption inside the fat layer was significantly lower (maximum SAR = 0.1 W/kg) than in the other parts of the biological tissue phantom.

3.3 Cumulative Temperature-Volume Histograms

The power of 69.5 W was needed to reach thr maximum of 43 °C for the temperature dependent blood perfusion model (scenario 1). Subsequently this power was also used for the other three scenarios. Cumulative temperature-volume histograms for all 4 scenarios are shown in Fig. 4. Cumulative temperature-volume histograms evaluate temperature distribution in the entire region of interest (in our case 100x100x40 mm^3). The highest temperature of 45.06 °C was obtained for scenario no. 4 which is caused by lower blood perfusion for muscle layer. The differences for maximal achieved temperature between scenarios 2 (42.44 °C) and 3 (42.71 °C) was 0.27 °C. Since these scenarios differ in blood perfusion for skin and fat layer we could expect the presence of an area with high temperature inside or in close proximity of fat.

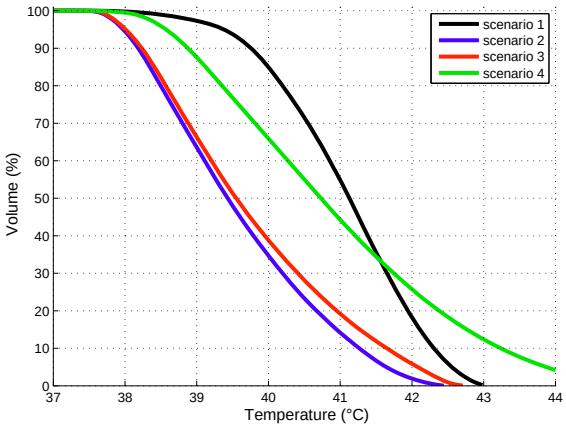

Fig. 4. Cumulative temperature-volume histogram for all scenarios applied identical power of 69.5 W.

Next, we tuned the input power to reach the maximum target temperature of 43 °C for every scenario. The corresponding P_{inc} are listed in Tab. 5.

Scenario	1	2	3	4
P_{inc} (W)	69.5	77.1	72.7	61.3

Tab. 5. Power necessary to reach maximum 43 °C.

Using this comparison it can be clearly seen that all scenarios with constant blood perfusion have similar 3D temperature distribution (maximal difference among scenarios 2 – 4 is within 0.1 °C) (see Fig. 5). Maximal temperature coverage difference between the scenario 1 and scenarios 2 – 4 was 1.58 °C for 70 % of target volume.

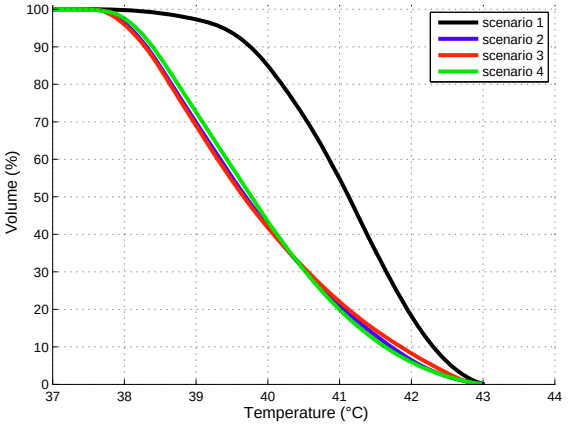

Fig. 5. Cumulative temperature-volume histogram, power scaled to reach 43 °C.

3.4 3D Temperature Distributions

The 3D temperature distribution for scenario 1 is shown in Fig. 6. Two planes perpendicular to the aperture had a cross section under the center of the aperture along the X axis where we expected the highest temperature (see Fig. 7). The 2D cross-section parallel to applicator aperture at the place where maximal temperature occurred (Fig. 8) (X = 13 mm under the surface) is also shown in Fig. 6.

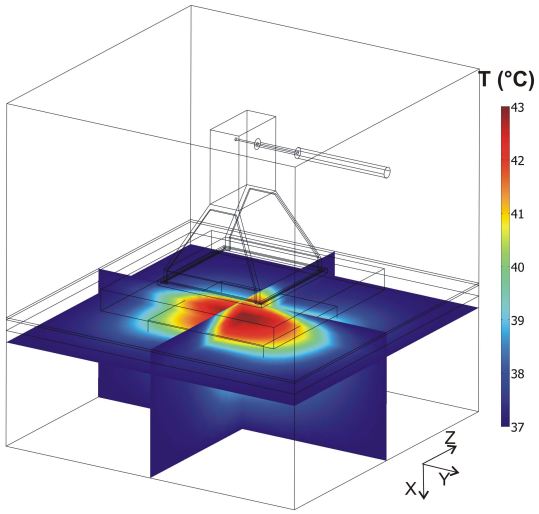

Fig. 6. 3D thermal profile for temperature dependent blood perfusion.

The positions of the maximum temperature points for all investigated scenarios varied from 13 mm to 15 mm under the phantom surface (see Fig. 7). Maximum temperatures were found in the muscle tissue in close proximity (1 – 3 mm) of fat layer. This depth can be varied changing water bolus temperature as introduced by Gaag et al. [22]. Inside the muscle tissue a maximum difference of 0.6 °C was found among the models with the constant blood perfusion (scenarios 2 – 4). We found a difference up to 2 °C at 40 mm depth between temperature dependent and constant blood perfusion models (scenarios 1 and 3). Temperature behavior in skin and fat was identical for scenarios 1 and 2.

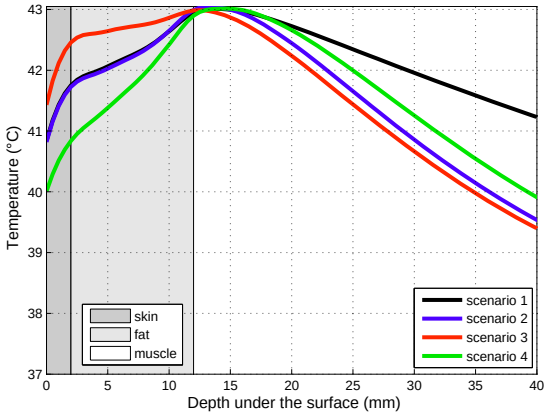

Fig. 7. Temperature profile along X axis.

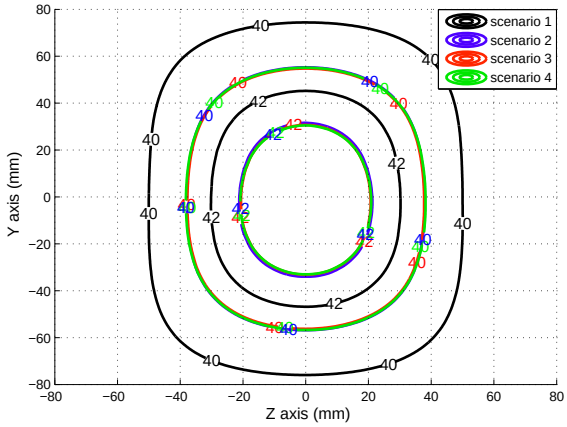

Fig. 8. 2D YZ temperature profile at depth of X = 13 mm for temperature contours 40 °C and 42 °C.

Fig. 8 shows the 2D (YZ) profile at the depth of X = 13 mm with temperature contours of 40 °C and 42 °C for all four scenarios. For this cross-section, all constant blood perfusion models have identical temperature distributions.

For the situation where maximum temperature of 43 °C was reached, we computed areas (cm^2) defined by temperature contours (TC) of 39 °C, 40 °C, 41 °C and 42 °C (Figs. 9, 10) as functions of depth under the surface. These areas were calculated from the 2D temperature cross sections (YZ) parallel to the surface. The area in Y and Z directions was not limited by the inner dimensions of the aperture (100x100 mm^2) as it was in the cases of cumulative temperatures volume histograms. Depth in the X direction varied in the range of 0 – 40 mm from the surface with a step of 1 mm.

Fig. 9 shows areas defined by temperature contours of 39 °C and 40 °C. Temperature dependent blood perfusion model (scenario 1) had largest $TC_{\geq 39\,^{\circ}\mathrm{C}}$ area of 193 cm^2 at the depth of X = 20 mm under the surface. For the constant blood perfusion models (scenarios 2- 4) areas of $TC_{\geq 39\,^{\circ}\mathrm{C}}$ were 107 cm^2 at the depth varied from 11 mm to 14 mm under the surface. For the $TC_{\geq 40\,^{\circ}\mathrm{C}}$ we reached almost two times larger maximum area for the scenario 1 (136 cm^2) in comparison with scenarios 2 – 4 (72 cm^2).

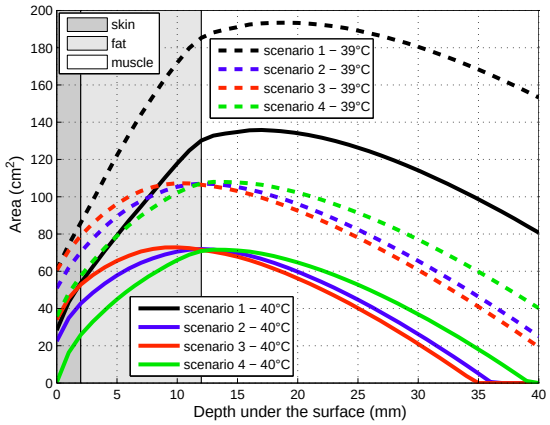

Fig. 9. Area (cm^2) defined with temperature contours of 39 °C (dashed line), 40 °C (solid line) for all 4 scenarios.

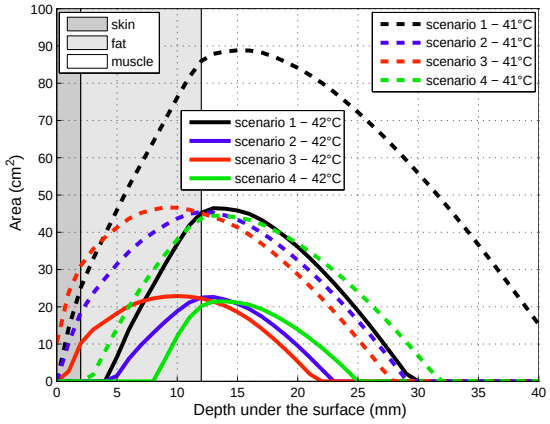

Fig. 10. Area (cm^2) defined with temperature contours of 41 °C (dashed line), 42 °C (solid line) for all 4 scenarios.

3.5 Calculation Time

Calculations were done using a standard desktop computer with Intel Pentium Core2Duo E8200 processor and 8GB of DDR2 (PC6400) RAM. We reached identical results using GMRES (generalized minimum residual solver) with geometric multigrid preconditier and direct PARADISO (parallel sparse direct solver). Computation time for constant perfusion models using direct PARADISO solver was 14 seconds and for GMRES 20 seconds. GMRES solver calculated nonlinear perfusion model in 116 seconds versus 209 seconds for direct PARADISO. These calculation times were in agreement with the assumption that direct PARADISO is more suitable for linear problems and GMRES more for nonlinear calculations.

4. Discussion

We cannot match prediction of 3D temperature profile for superficial hyperthermia using constant and temperature dependent blood perfusion. All scenarios with constant blood perfusion had identical (maximal difference of 0.1 °C) cumulative temperature-volume histograms for the models where we reached the maximum temperature of 43 °C.

Hence a different constant blood perfusion does not change the relative 3D temperature distribution but only its absolute values. Thus the only difference was in power required to reach 43 °C which represents just a scaling factor and has no influence on the spatial temperature distribution. For the temperature dependent blood perfusion model 85 % of the studied volume was covered in a temperature higher or equal than 40 °C that in comparison with 43 % for constant blood perfusion clearly describes the differences between these scenarios (Fig. 5).

51.3 % of the power entering the calculation domain was absorbed inside the deionized water filling of the applicator which was 13.3 % higher than what Bruijne et al. found using LCA [27]. This will influence the applicator efficiency defined as a relationship between P_{inc} and the amount of power absorbed inside the biological tissue equivalent phantom. Low efficiency of the applicators will result in higher requirements for the output power from microwave generators.

For all the studied scenarios the position of the maximum temperature remained in the muscle layer in close proximity to the fat layer (13 – 15 mm under the surface) which is in agreement with the results of Gaag et al. [22]. Gaag et al. used constant blood perfusion scaled to the averaged values proposed by Lang et al. [19]. Modeling of blood perfusion as temperature dependent quantity does not change this position. Our findings verified the work of Gaag et. al. [22] also for temperature dependent blood perfusion model.

We selected the dimensions of the biological tissue equivalent phantom model to be large enough to avoid influence of boundaries in thermal calculations. All boundaries inside the model were set to the temperature of 37 °C. Such boundaries' conditions could be counted as thermal sources that could influence the resulting 3D temperature distribution. To verify this assumption we also calculated a model with thermal insulation boundary conditions, ensuring that no temperature is removed from the calculation domain. Since the maximum 3D temperature difference between these two models was 0.0048 °C we conclude that boundary set at 37 °C had no influence on the temperature profile inside the region of interest.

We modeled influence of the water bolus as a boundary condition with a heat transfer coefficient h = 152 W m^{-2}K^{-1}. This value was found by Gaag et. al as the best agreement between simulated and measured data for the single LCA. In our simulations this value was constant along the area where water bolus was in contact with the treated area so we expected homogeneous flow through the entire volume of the water bolus. This assumption does not need to be true especially at the corner of the water bolus. Adequate study can be done to asses the flow inside the water bolus with respect to the real configuration of the water inflow and outflow [28].

5. Conclusion

The blood perfusion in temperature calculations for superficial hyperthermia should be treated as a temperature dependent quantity. For the treatment planning based on the prediction of temperature distribution it is essential to validate temperature dependent blood perfusion model with the clinical data. The knowledge of perfusion changes during treatment due to the temperature enhancement is very limited. If interstitial thermometry (invasive inside catheters) is present during superficial treatment, the thermal wash-out effect (after steady state is reached) can be used as measure for the local blood perfusion [25]. These values could be used for prediction of 3D temperature profile with realistic blood perfusion values. The other possibilities is to use magnetic resonance imagining (MRI) for 3D temperature noninvasive measurement [29]. Afterwards, optimization of blood perfusion term and thermal conductivity in BHTE could be used to match the predicted and the measured 3D temperature profiles. MRI can also be used for direct measurement of the 3D perfusion profile [30]. Nevertheless the usage of MRI in clinic cannot be included to a standardized treatment procedure for its high cost and the necessity to adapt treatment technique to use with MRI.

Acknowledgments

This research was supported by Grant Agency of the Czech Republic (102/08/H081), by the Ministry of Education, Youth and Sports of the Czech Republic (MSM6840770012) and by the Dutch Cancer Society (EMCR2007-3837).

References

[1] OVERGAARD, J., GONZALEZ GONZALEZ, D., HULSHOF, M. C. C. H., ARCANGELI, G., DAHL, O., MELLA, O., BENTZEN, S. M. Hyperthermia as an adjuvant to radiation therapy of recurrent or metastatic malignant melanoma. A multicentre randomized trial by the European Society for Hypertermic Oncology. *International Journal of Hyperthermia*, 2009, vol. 25, no. 5, p. 323 – 334.

[2] VAN DER ZEE, J., OVERGAARD, J. Hyperthermia classic commentary: 'Hyperthermia as an adjuvant to radiation therapy of recurrent or metastatic malignant melanoma. A multicentre randomized trial by the European Society for Hyperthermic Oncology' by J. Overgaard, D. González González, M.C.C.H. Hulshof, G. Arcangeli, O. Dahl, O. Mella & S.M. Bentzen, International Journal of Hyperthermia 1996;12:3–20. *International Journal of Hyperthermia*, 2009, vol. 25, no. 5, p. 335 – 337.

[3] VERNON, C. C., HAND, J. W., FIELD, S. B., MACHIN, D., WHALEY, J. B., VAN DER ZEE, J., VAN PUTTEN, W. L. J., VAN RHOON, G. C., VAN DIJK, J. D. P., GONZALEZ, D. G., LIU, F., GOODMAN, P., SHERAR, M. Radiotherapy with or without hyperthermia in the treatment of superficial localized breast cancer: Results from five randomized controlled trials. *International Journal of Radiation Oncology Biology Physics*, 1996, vol. 35, no. 4, p. 731 – 744.

[4] JONES, E., OLESON, J. R., PROSNITZ, L. R., SAMULSKI, T. V., VUJASKOVIC, Z., YU, D., SANDERS, L. L., DEWHIRST, M. W. Randomized trial of hyperthermia and radiation for superficial tumors. *Journal of Clinical Oncology*, 2005, vol. 23, no. 13, p. 3079 – 3085.

[5] FRANCKENA, M., STALPERS, L., KOPER, P., WIGGENRAAD, R., HOOGENRAAD, W., VAN DIJK, J., WÁRLÁM-RODENHUIS, C., JOBSEN, J., VAN RHOON, G., VAN DER ZEE, J. Long-term improvement in treatment outcome after radiotherapy and hyperthermia in locoregionally advanced cervix cancer: An update of the Dutch Deep Hyperthermia Trial. *International Journal of Radiation Oncology Biology Physics*, 2008, vol. 70, no. 4, p. 1176 – 1182.

[6] ARUNACHALAM, K., MACCARINI, P., JUANG, T., GAETA, C., STAUFFER, R. P. Performance evaluation of a conformal thermal monitoring sheet sensor array for measurement of surface temperature distributions during superficial hyperthermia treatments. *International J. Hyperthermia*, 2008, vol. 24, no. 4, p. 313 – 325.

[7] VAN DER ZEE, J., RIETVELD, P. J. M., BROEKMEYER-REIRINK, M. P., WIELHEESEN, D. H. M., VAN RHOON, G. C. Hyperthermia in recurrent breast cancer: From experimental oncology to standard practice. *Experimental Oncology*, 2002, vol. 24, no. 1, p. 45 – 50.

[8] DE BRUIJNE, M., WIELHEESEN, D. H. M., VAN DER ZEE, J., CHAVANES, N., VAN RHOON, G. C. Benefits of superficial hyperthermia treatment planning: Five case study. *International Journal of Hyperthermia*, 2007, vol. 23, no. 5, p. 417 – 429.

[9] STAUFFER, P. R. Evolving technology for thermal therapy of cancer. *International Journal of Hyperthermia*, 2005, vol. 21, no. 8, p. 731 – 744.

[10] VAN RHOON, G. C., RIETVELD, P. J. M., VAN DER ZEE, J. A 433 MHz Lucite cone waveguide applicator for superficial hyperthermia. *International Journal of Hyperthermia*, 1998, vol. 14, no. 1, p. 13 – 27.

[11] RIETVELD, P. J. M., PUTTEN, W. L. J., VAN DER ZEE, J., VAN RHOON, G. C. Comparison of the clinical effectiveness of the 433 MHz Lucite cone applicator with that of a conventional waveguide applicator in applications of superficial hyperthermia. *International Journal of Radiation Oncology Biology Physics*, 1999, vol. 43, no. 3, p. 681 – 687.

[12] GELVICH, E. A., MAZOKHIN, V. N. Contact flexible microstrip applicators (CFMA) in a range from microwaves up to short waves. *IEEE Transaction on Biomedical Engineering*, 2002, vol. 49, no. 9, p. 1015 – 1023.

[13] KOK, H. P., DE GREEF, M., CORREIA, D., ZUM VÖRDE SIVE VÖRDING, P. J., VAN STAM, G., GELVICH, E. A., BEL, A., CREZEE, J., FDTD simulations to asses the performance of CFMA-434 applicators for superficial hyperthermia. *International Journal of Hyperthermia*, 2009, vol. 25, no. 6, p. 462 – 476.

[14] STAUFFER, P. R., ROSSETTO, F., LEONCINI, M., GENTILLI, G. B., Radiation patterns of dual concentric conductor microstrip antennas for superficial hyperthermia. *IEEE Transaction on Biomedical Engineering*, 1998, vol. 45, no. 5, p. 605 – 613.

[15] JOHNSON, J. E., NEUMAN, D. G., MACCARINI, P. F., JUANG, T., STAUFFER, P. R., TURNER, P. Evaluation of a dual-arm archimedean spiral array for microwave hyperthermia. *International Journal of Hyperthermia*, 2006, vol. 22, no. 6, p. 475 – 490.

[16] VAN WIERINGEN, N., WIERSMA, J., ZUM VÖRDE SIVE VÖRDING, P. J. , OLDENBORG, S., GELVICH, E. A., MAZOKHIN, V. N., VAN DIJK, J. D. P., CREZEE, J. Characteristic and performance evaluation of the capacitive Contact Flexible Microstrip Applicator operating at 70 MHz for external hyperthermia. *International Journal of Hyperthermia*, 2009, vol. 25, no. 7, p. 542 – 553.

[17] PENNES, H. H. Analysis of tissue and arterial blood temperatures in the resting human forearm. *Journal of Applied Physiology*, 1948, vol. 1, no. 2 p. 93 – 122.

[18] CREZEE, J., LAGENDIJK, J. J. W. Experimental verification of bioheat transfer theories: measurement of temperature profiles around large artificial vessels in perfused tissue. *Physics in Medicine and Biology*, 1990, vol. 35, no. 7, p. 905 – 923.

[19] LANG, J., ERDMANN, B., SEEBASS, M. Impact of nonlinear heat transfer on temperature control in regional hyperthermia. *IEEE Transaction on Biomedical Engineering*, 1999, vol. 46, no. 9, p. 1129 – 1138.

[20] SONG, CH. W., LOKSHINA, A., RHEE, J. G., PATTEN, M, LEVITT, S. H. Implication of blood flow in hyperthermia treatment of tumours. *IEEE Transaction on Biomedical Engineering*, 1984, vol. 31, no. 1, p. 9 – 16.

[21] COMSOL Multiphysics 3.5a. Stockholm (Sweden): COMSOL AB, 2008.

[22] VAN DER GAAG, M. L., DE BRUIJNE, M., SAMARAS, T., VAN DER ZEE, J., VAN RHOON, G. C. Development of a guideline for the water bolus temperature in superficial hyperthermia. *International Journal of Hyperthermia*, 2006, vol. 22, no. 8, p. 637 – 656.

[23] DE BRUIJNE, M., SAMARAS, T., BAKKER, J. F., VAN RHOON, G. C. Effects of water bolus size, shape and configuration on the SAR distribution pattern of the Lucite cone applicator. *International Journal of Hyperthermia*, 2006, vol. 22, no. 1, p. 15 – 28.

[24] GABRIEL, S., LAU, R. W., GABRIEL, C. The dielectric properties of biological tissues: III. Parametric models for the dielectric spectrum of tissues. *Physics in Medicine and Biology*, 1996, vol. 41, no. 11, p. 2271 – 2293. [Online] Available at: http://niremf.ifac.cnr.it/tissprop/

[25] *Treatment Planning and Modeling in Hyperthermia (technical report)*. COMAC BMR Task Group Report. Rome (Italy): University of Rome, 1992.

[26] KUMARADAS, J. C., SHERAR, M. D. Edge-element based finite element analyses of microwave hyperthermia treatments for superficial tumours on the chest wall. *International Journal of Hyperthermia*, 2003, vol. 19, no. 4, p. 414 – 430.

[27] DE BRUIJNE, M., SAMARAS, T., CHAVANNES, N., VAN RHOON, G. C. Quantitative validation of the 3D SAR profile of hyperthermia applicators using the gamma method. *Physics in Medicine and Biology*, 2007, vol. 46, no. 14, p. 3075 – 3088.

[28] ARUNACHALAM, K., MACCARINI, P. F., SCHLORFF, J. L., BIRKELUND, Y., JACOBSEN, S., STAUFFER, P. R. Design of a water coupling bolus with improved flow distribution for multi-element superficial hyperthermia applicators. *International Journal of Hyperthermia*, 2009, vol. 25, no. 7, p. 554 – 565.

[29] WYATT, C., SOHER, B., MACCARINI, P., CHARLES, H. C., STAUFFER, P., MACFALL, J. Hyperthermia MRI temperature measurement: Evaluation of measurement stabilisation strategies for extremity and breast tumours. *International Journal of Hyperthermia*, 2009, vol. 25, no. 6, p. 405 – 415.

[30] LÜDEMANN, L., WUST, P., GELLERMANN, J. Perfusion measurement using DCE-MRI: Implication for hyperthermia. *International Journal of Hyperthermia*, 2008, vol. 24, no. 1, p. 91 – 96.

About Authors...

Tomáš DŘÍŽĎAL received the MSc. degree from Czech Technical University in Prague in 2005. Since 2005 he has been a postgraduate student at the Department of Electromagnetic Field, Czech Technical University in Prague, Czech Republic. He is currently working towards the Ph.D. degree at the Department of Radiotherapy, Erasmus MC–Daniel den Hoed Cancer Center, Rotterdam, The Netherlands. His main field of interest is a superficial hyperthermia.

Paolo Togni received MSc. degree in electronic engineering from Politecnico di Milano in 2004 . In 2009 he received the PhD degree from Czech Technical University in Prague at the Department of Electromagnetic Field, with his topic in microwave applicators for medical and biological purposes. He is currently working as physicist in hyperthermia unit of the Department of Radiotherapy, Erasmus MC Daniel den Hoed Cancer Center, Rotterdam, The Netherlands. His main fields of interest are applicators and systems for regional hyperthermia.

Lukáš VÍŠEK was born in Vysoke Myto in 1982 and received his MSc. degree from Czech Technical University in Prague in February 2006. He is currently a postgraduate student at the Department of Electromagnetic Field at Faculty of Electrical Engineering. His main present work deals with exposure system development for unrestrained small animals which will serve for research of non-thermal effects of electromagnetic fields and hyperthermic applicators.

Jan VRBA received the MSc. and PhD. degrees from the CTU in Prague and since 1993 he has been a professor at the Department of Electromagnetic Field, Czech Technical University in Prague. His research has been focused on medical and industrial applications of microwave technology.